AD-750 379

AN ANALYSIS OF 5.56MM ALUMINUM CARTRIDGE CASE BURN-THROUGH PHENOMENON

Walter H. Squire, et al

Frankford Arsenal
Philadelphia, Pennsylvania

1972

425

SQUIRE AND DONNARD

AD 750 379

AN ANALYSIS OF 5.56mm ALUMINUM CARTRIDGE CASE "BURN-THROUGH" PHENOMENON

WALTER H. SQUIRE AND REED E. DONNARD
FRANKFORD ARSENAL
PHILADELPHIA, PA.

INTRODUCTION: The United States Army - SASA, MUCOM, and Frankford Arsenal - is engaged in an exploratory development program to determine the engineering parameters required to utilize aluminum cartridge cases in high-pressure, small-caliber ammunition systems. This work is based on the need to create lightweight ammunition/weapon systems in near future applications. Conservation of copper resources is an added benefit to be gained from success in this effort.

To date, a significant fact which has precluded the acceptance of aluminum cartridge cases in the logistic system is the nature of the failure process - heretofore identified as "burn-through". When a mechanical case failure is encountered during the firing of aluminum-cased ammunition, particularly with high-pressure, high-performance weapon systems, the failure of an aluminum cartridge case is characterized by a large efflux of very luminous gases at the breech of the weapon, the serious erosion of the cartridge case, and often, the inability of the weapon to function properly thereafter. Thus, this failure may result in serious harm to the rifleman and damage the weapon.

In order to investigate the failure dynamics, as a basis for finding a solution or solutions to this problem, it was found that a small hole drilled in the head region of an aluminum cartridge case, or a four thousands deep longitudinal scratch would, upon firing, result in "burn-through". As a result of this simulation of the failure process, it was concluded that a gas path must be available for the otherwise unrestricted flow of propellant gases from the interior of the cartridge case through the path in the case wall and to the atmosphere. Figure 1 is a photograph of the results of firing brass and aluminum cartridge cases with a 0.0135 inch (diameter) hole in the head region of each case. The two brass cases seem unaffected after firing. However, the two aluminum cartridge cases show the typical erosion in the head region; the unfired aluminum cartridge

Begin

15

case can be used to compare the damage after firing with its initial, drilled condition. This paper is addressed to a discussion concerning the peculiar results when propellant gases are allowed to pass through an induced fissure in an aluminum cartridge case.

STATEMENT OF THE PROBLEM: Using a pre-placed gas path in an aluminum cartridge case as a vehicle to study this phenomenon, the mathematics which follow describe the heat flux resulting from the fast moving propellant gases through the induced orifice and allow determination of the temperature profiles in selected regions of the cartridge case. Emphasis is placed on the gas/solid interface - the interior surface of the induced orifice. To test the accuracy of the mathematical model, the appropriate physical constants of the case materials under consideration, along with values obtained from an experimental program, were substituted into the equations. Temperature profiles and total erosion values were thus calculated. This analytical tool was used to investigate the premise that portions of the aluminum cartridge case undergo melting and that the total amount of aluminum ablated from the cartridge case is correctly predicted by a classical melting theory. The same mathematics, when applied to the flow through a brass cartridge case, should indicate minimal metal removal.

In order to facilitate a closed-form solution of the mathematical model, the following assumptions were employed:

(1) The dimensions of the induced orifice remain constant until melting,

(2) Propellant gas behaves as an ideal gas,

(3) Classical heat conduction equation describes the dissipation of energy in the solid until melting,

(4) The physical properties of the cartridge case material are constant during the experiment,

(5) It is possible to identify an average operating pressure (P_o = 25,000psi), and

(6) The gas temperature is the adiabatic flame temperature (T_o = 5040°R).

EXPERIMENTAL: One portion of the experimental program involved pre-placing holes of various sizes in the head region of aluminum cartridge cases. The cases were loaded with various charges of conventional ball propellant thereby providing a range of peak chamber pressures. A quantitative measure relating peak chamber pressure and initial hole size to "burn-through" was obtained by weighing the cases before and after firing thus determining the amount of metal lost as a result of "burn-through".

Two other pieces of experimental information were needed. To obtain pressure vs time data a thick-walled test barrel was drilled and threaded to accept a 607A Kistler Gauge. This gauge was positioned midway along the longitudinal axis of the cartridge case to measure the gas pressure. Figure 2 shows the pressure-time history of

the propellant gases inside a 5.56mm cartridge case which contained the charge of 27.0 grains of WC846 propellant.

In addition to the pressure-time curve, it was desired to monitor the initiation and the duration of the gas flow from the orifice. Hence, positioning a photoelectric cell in the same horizontal plane and at right angles to the induced orifice provided the desired information. That is, by recording the output of the photoelectric cell on the screen on an oscilloscope, it is possible to determine when the gases first exit the orifice and for how long the flow continues.

ANALYSIS: The mathematical analysis is directed to that portion of the cartridge case shown in Figure 3. Since the hole is drilled in the most massive region of the case, and since the length to diameter (L/D) ratio of the hole is approximately 5, a reasonable approximation to the region of the case where the hole is drilled is that of a small hole in a medium of infinite extent in the radial direction. Distance along the axis of the bore is specified by the variable z, and distance from the center line of the bore in the radial direction is given by the variable r.

It is first necessary to describe the flow of propellant gases from the interior of the cartridge case through the induced fissure. To do so, it is important to select the most representative gas dynamic model, based upon bore size. With a L/D ratio of approximately 5, the relatively small opening of 0.0135 inch in diameter, and the rapid rate of pressurization, the flow may be assumed to be choked. The additional assumption is made that the flow is developed to the point where it consists of a well defined boundary layer and a central, core region. Figure 4 is a drawing depicting this flow process. The temperature, pressure, density, and velocity as a function of position in the core region can be determined with the appropriate flow model. Determination of the nature of the boundary layer, laminar or turbulent, can be accomplished by an examination of the magnitude of the local Reynolds number.

Lee and Sears (1) suggest an adiabatic treatment of the flow be considered providing the bore is not too long (less than ten bore diameters). Admittedly, the flow process should account for the substantial transfer of energy to the bore's sidewalls since melting has been hypothesized to occur. The adiabatic assumption of the flow does not contradict the hypothesized fact that there is substantial energy transfer. The analysis of the core region merely permits a determination of the gas conditions - i.e. temperature, pressure, density, and velocity - external to the boundary layer. It must be remembered that it is across the boundary layer that the energy is transferred to the bore's sidewalls. Thus, the gas dynamics in the core will be treated as adiabatic flow with friction in a duct of constant area.

Shapiro (2) has developed a series of working formulas to describe such a flow process. Momentum, energy, and mass equations are written for the flow of a perfect gas through an elemental control volume. Since the reservoir (chamber) conditions are available and since choking is assumed to occur at the exit, these formulas may be used to predict the temperature, pressure, velocity, and density at any position along the bore's axis.

The Mach number as a function of position along the bore's axis must first be determined. Lee and Sears (1) give a relationship for the bore length L, required for the flow to pass from a Mach number, M_1, to a Mach number, M_2, as

$$\frac{4fL}{D} = \frac{4f}{D}(L_{max})_{M_1} - \frac{4f}{D}(L_{max})_{M_2} \qquad (1)$$

where f is the friction factor, and
D is the diameter of the bore.

The friction factor, f, is defined by the Reynolds analogy as

$$f = \frac{2h_{c_x}}{\rho v C_p} \qquad (2)$$

where h_{c_x} is the heat transfer coefficient
ρ is the gas density
v is the gas velocity, and
C_p is the specific heat as constant pressure.

Since at this point in the analysis, values for h_{c_x}, ρ and v are all unknown, a value for the friction factor must be assumed. An iterative technique can be used later to identify a correct friction factor, once more information on the fluid properties within the central core region is available. Shapiro (2) states that friction factors in the range of 0.001 to 0.004 are realistic for the type of flow with which this analysis is concerned. Keenan and Kaye's (3) gas tables for the adiabatic flow of a perfect gas through a constant area duct with friction, in conjunction with equation (1), are used to determine the Mach number as a function of position throughout the bore for friction factors of 0.001, 0.002, and 0.004. These data are presented in Figure 5.

Now that the local Mach number is available, it is possible to evaluate both the free stream and stagnation values for the temperature, pressure, and density at any point along the bore's axis. The chamber conditions - those describing the combustion of the propellant grains inside the cartridge case - to be used throught this analysis are:

$T_o = 5040°R$, $P_o = 2.5 \times 10^4$ psi, $R = 64.372$ ft-lb$_f$/ lb$_m$ °R
$\rho_o = 11.09$ lb$_m$/ft^3, and $\gamma = 1.24$.

To obtain the gas properties at the beginning of the bore - the inlet, an isentropic process is thought to be valid. Shapiro (2) provides the following governing equations for an isentropic process:

$$T_\infty = \frac{T_o}{1 + \frac{\gamma-1}{2} M^2} \tag{3}$$

$$P_\infty = \frac{P_o}{\left(1 + \frac{\gamma-1}{2} M^2\right)^{\gamma/\gamma-1}} \tag{4}$$

$$\rho_\infty = \frac{\rho_o}{\left(1 + \frac{\gamma-1}{2} M^2\right)^{1/\gamma-1}} \tag{5}$$

where the free stream conditions and the stagnation states are identified by the subscripts ∞ and o respectively. The local value for the gas velocity may also be determined from formula

$$V = M\sqrt{\gamma R T_\infty} \,. \tag{6}$$

In order to determine the axial dependency of the free stream temperature, pressure, density, and velocity, equations (3), (4), (5), and (6) are again used. The appropriate value for the local Mach number is obtained from Figure 5. These calculations are performed for a friction factor of 0.002 at positions where the Mach numbers are 0.90, and 0.95, and 1.00 and are shown in Figure 6. Although a detailed treatment of the fluid mechanics has been addressed, Figure 6 shows that the free stream conditions do not vary appreciably along the axis of the bore.

The problem which is being studied is that of flow and heat transfer in a small bore. Kreith (4) states that for very short tubes or rectangular ducts with initially uniform velocity and temperature distribution, the flow conditions along the wall approximate those along a flat plate. Hence, the original two dimensional cylindrical geometry (r,z) can be replaced with a two dimensional cartesian system (x,y). Further justification for the flat plate treatment of the problem may be obtained by showing that the boundary layer displacement thickness is small compared to the bore's radius. This fact implies that the boundary layer is essentially localized near the surface of the bore.

To determine the nature of the boundary layer, turbulent or laminar, the local Reynolds number is needed. The Reynolds number, based on length, is given by $Re_z = V\rho z/\mu$ where the values of the velocity, V, and the gas density, ρ, for a particular value of z are obtained from Figure 6 and the absolute viscosity, μ, is 4.72×10.5^{-5} lb_m/ ft-sec. Kreith (4) reports that the flow over a flat plate is turbulent where the local Reynolds number is approximately 3×10^5. Comparing 3×10^5 with the calculated values of 1.26×10^6 ($Re_{z=0.030\ inch}$) and 2.40×10^6 ($Re_{z=0.062\ inch}$), it is concluded that the flow is indeed turbulent.

It is now possible to calculate the boundary layer thickness at

any point along the axis of the bore. Rohsenow and Choi (5) report that the boundary layer thickness, δ, for turbulent flow is

$$\delta = \frac{0.37\, z}{(Re_z)^{1/5}} . \tag{7}$$

For the flat plate assumption to be valid it is necessary to show

$$\frac{\delta^*}{a} \ll 1 \tag{8}$$

where a is the bore's radius and δ^* is the boundary layer displacement thickness. Olson (6) states that the boundary layer displacement thickness for turbulent flow is given by $\delta/8$; hence, equations (7) and (8) may be combined and evaluated. For example, at z =0.031 inch the bore's midpoint δ^*/a is 0.0128, which is very much less than one, thereby justifying the flat plate treatment of the bore's surface.

The energy transport to the bore's sidewall occurs principally by forced convection. The effect of radiation can be shown to contribute little to the net heat flux. It is therefore important to define the Nusselt number in terms of the Prandtl and Reynolds numbers. With turbulent flow over a flat plate, Olson (6) states that a reasonable value for the Nusselt number may be obtained from

$$Nu_z = 0.0288\,(P_r)^{1/3}(Re_z)^{4/5} \tag{9}$$

where Nu_z implies that the Nusselt number is a function of position along the bore's longitudinal axis. Combining equation (9) with the classical definition of the Nusselt number, $Nu_z = h_c z / k_g$, where k_g is the thermal conductivity of propellant gas, it is possible to identify the convective heat flux to the bore's sidewall as

$$q_0 = \frac{0.0288\,(P_r)^{1/3}(Re_z)^{4/5} k_g}{z}(T_s - T_g) \tag{10}$$

where T_g is a characteristic gas temperature and T_s is the surface temperature of the solid. The gas properties used in the evaluation of the Reynolds and Prandtl numbers must be evaluated at a reference temperature, T^*, determined empirically by Eckert (7) to be

$$T^* = T_\infty + 0.50(T_0 - T_\infty) + 0.22(T_{a.w.} - T_\infty).$$

Consideration of the recovery factor permits substitution of the adiabatic wall temperature, $T_{a.w.}$, by the stagnation temperature so that the above equation becomes

$$T^* = T_\infty + 0.72(T_0 - T_\infty).$$

The heat flux described by equation (10) is incident to the bore's sidewalls. By showing that the thermal layer does not penetrate the solid to any significant depth during the interior ballistic cycle, it is possible to treat the conduction problem as a one dimensional slab instead of as a region exterior to a cylindrical hole of diameter, D, and extending to infinity in the radial direction. The heat conduction is then reduced to a one dimensional,

time-dependent problem subject to a Newton's Law of Cooling boundary condition of the third kind. Rohsenow and Choi (5) provide a solution to such a problem and further point out that the heating of a thick body by a hot fluid at the surface approximates this case during the early stages of the transient. Their solution is as follows

$$\frac{T_s - T_i}{T_g - T_i} = \left[\operatorname{erfc}\left(\frac{x}{2\sqrt{\chi t}}\right) - \exp\left(\frac{x h_{c_2}}{k_s} + \frac{\chi t}{(k_s/h_{c_2})^2}\right) \operatorname{erfc}\left(\frac{x}{2\sqrt{\chi t}} + \frac{\sqrt{\chi t}}{(k_s/h_{c_2})}\right)\right] \quad (11)$$

where χ and k_s, are the thermal diffusivities and conductivities of the metal in question, T_i is the initial temperature of the solid, and t is the time variable.

DISCUSSION: The analytical model, developed previously and culminating in equation (11), allows determination of the bore surface temperature given gas flow. To investigate the performance of brass and aluminum alloy cartridge cases, it is a simple matter to substitute the appropriate physical parameters - χ and k_s - and calculate the surface temperature at several axial positions as was done to prepare Figures 7 and 8. Figure 7 implies that the surface of an aluminum bore ($\chi = 0$) reaches the melting temperature after approximately 0.35 milliseconds; the brass bore's melting temperature (Figure 8) is approached only late in the interior ballistic cycle.

To predict the total amount of metal removed during a "burn-through", equation (11) is solved using a forward difference-in-time technique with the additional condition that for any point to be removed, it must realize a local temperature equal to the melting temperature plus an additional amount of heat to cause an elemental mass, Δm, to liquify. Therefore, the total heat flux required to cause melting, hence metal removal, will be

$$q_{removed} = \Delta m C_p (T_{melt} - T_i) + \Delta m H_f \quad (12)$$

where H_f is the heat of fusion. Figure 9 shows the results of such an exercise (labeled classical melting) and the results of an experimental effort wherein the amount of metal lost during "burn-through" has been correlated with peak chamber pressure. A comparison shows that the experimental results are not predicted entirely by a classical melting theory.

In order to determine if any additional energy sources were present during an aluminum cartridge case "burn-through", high speed motion pictures and still photographs were taken of this phenomenon. Figure 10(a) shows the characteristic plume resulting from propellant gases, generated in a combustor, passing through a 0.0135 inch (diameter) hole in an aluminum test specimen. This discharge has been channeled into a plexiglas cylinder and produces a bright incandescence throughout the entire cylinder. However, when the cylinder was flushed with nitrogen, the major portion of the gaseous discharge has been quenched as is shown in Figure 10(b). All that remains as a result of the inert atmosphere is a small localized region in close

proximity to the specimen. It is interesting to note that although a major portion of the discharge has been eliminated by the nitrogen atmosphere, the damage (metal removal) inflicted to each test specimen is the same. Also, it is apparent that the "burn-through" plume occurs in two separate phases - a large secondary cloud existing exterior to the aluminum specimen (identified as the oxidation of aluminum to aluminum oxide) and a localized primary reaction zone existing in close proximity to the specimen (possibly a vapor phase reaction between aluminum and the combustion gases). Hence, the localized primary reaction zone is responsible for additional metal removal and must be considered in the mathematical model.

To determine the magnitude of the heat flux resulting from the primary reaction zone, a double disk arrangement of aluminum and brass test specimens was used in the combustor. There were two variations of this experiment. First, the aluminum was placed closest to the combustor and the brass faced the atmosphere. In the second experiment, the orientation of the two test specimens was reversed. The data obtained from this experiment are shown in Figure 11. It is possible to account for the drastic differences in these data. If the aluminum disk first witnesses flow of propellant gas, the localized exothermic reaction will be exposed to the brass specimen. The final result being that the brass specimen is exposed to much more heat flux than would be expected if the aluminum specimen were not present. If, on the other hand, the propellant gas first passes through the brass specimen and then the aluminum, the exothermic reaction associated with the aluminum will be carried (by the fast moving propellant gas stream) to the atmosphere. There will be no material on which the exothermic reaction can act. By measuring the amount of metal removed from the brass specimen under both cases of the experiment and by using equation (12), it is possible to calculate the additional energy flux to the brass specimen as a result of the exothermic reaction. The brass specimen, in a sense, is being used as a calorimeter for the primary reaction occurring with the aluminum specimen. Once determined, this additional energy flux is used as a corrective factor to the melting theory. Figure 12 shows a comparison between the experimental results and the theoretical predictions when augmented by the heat flux from the primary reaction zone. The agreement is favorable.

CONCLUSIONS: This work was aimed at understanding the "burn-through" problem that has impeded orderly engineering development and application of aluminum alloy cartridge cases in high-performance ammunition since the 1890's. It has been shown that a gas path through the wall of an aluminum case, and through which propellant gas can flow during the internal ballistic cycle, is a precursor to the "burn-through" phenomenon. Once this gas path has been established in an aluminum cartridge case, melting of the path surface starts early in the flow cycle. On the other hand, the melting point of a similar surface in a brass case is only approached late in the cycle. Hence, the key factor in an aluminum cartridge case, is the onset of melting early in the interior ballistic cycle. This melting

is almost instantaneously followed by primary, exothermic chemical reactions of propellant gas molecules with available aluminum alloy material. This exothermically aggravates the ablation of the aluminum case surface and adjacent steel weapon surfaces over which the conglomerate molten and reacting material flows. This primary reaction is followed by a secondary reaction which consists of the oxidation of unreacted case material that is blown into the atmosphere

Armed with this knowledge, solutions to this problem have been found that either prevent propellant gas flow through a path in the case that develops unintentionally during firing of the ammunition, or alter the effect of propellant gas flow through such a gas path. Since an engineering understanding of the "burn-through" phenomenon is available, work is currently underway to demonstrate the feasibility of aluminum cartridge cases thereby advancing the program from exploratory development to advanced engineering development.

REFERENCES:

1. Lee, J.F., and Sears, F.W., Thermodynamics, Addison-Wesley, Cambridge, Mass., 1955.

2. Shapiro, A.H., The Dynamics and Thermodynamics of Compressible Fluid Flow, Vol. I, Ronald Press, New York, 1953.

3. Keenan, J.H., and Kaye, J., Gas Tables, Wiley, New York, 1956.

4. Kreith, F., Principles of Heat Transfer, International Textbook Company, Scranton, Penna., 1963.

5. Rohsenow, W.M., and Choi, H., Heat, Mass, and Momentum Transfer, Prentice-Hall, Englewood Cliffs, New Jersey, 1961.

6. Olson, R.M., Essentials of Engineering Fluid Mechanics, International Textbook Company, Scranton, Penna., 1962.

7. Eckert, E.R.G., Transactions of the American Society of Mechanical Engineers, Vol. 78, 1956.

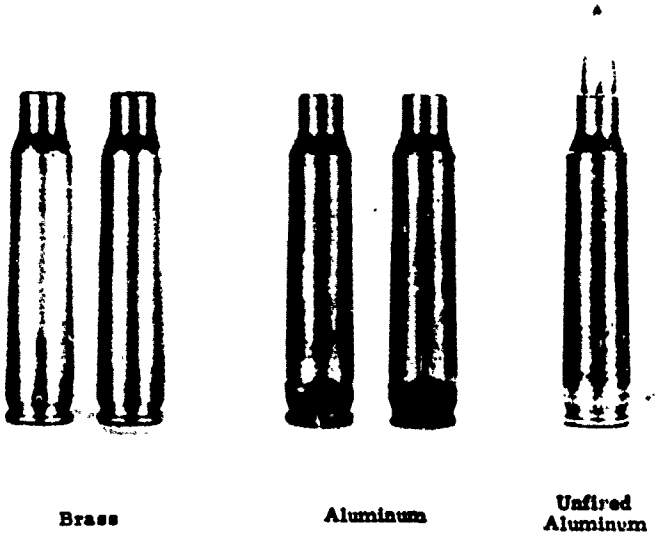

Figure 1. Drilled Hole Experiment

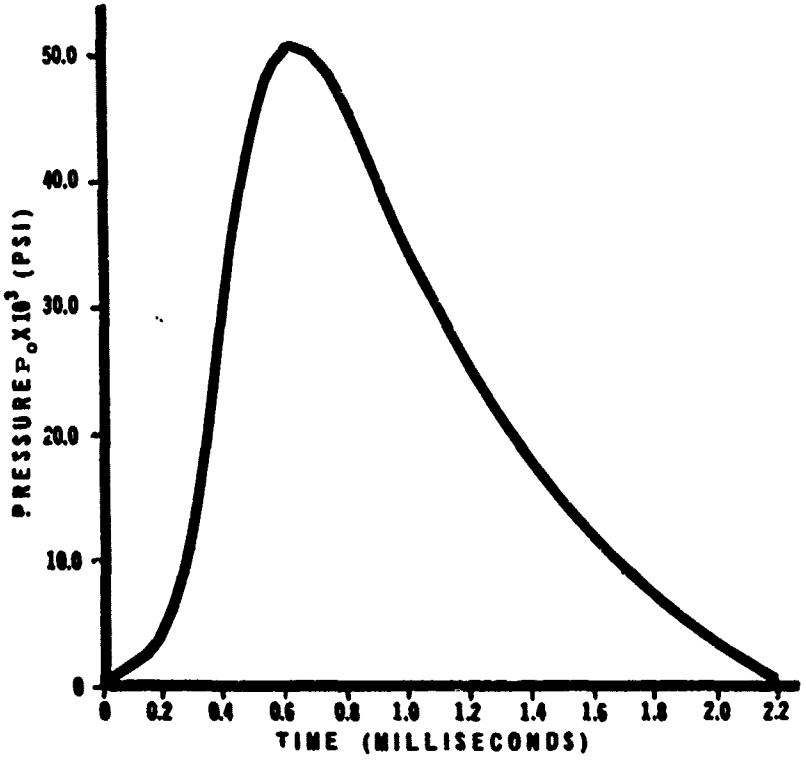

Figure 2. Pressure vs Time for Standard Charge in Aluminum Case

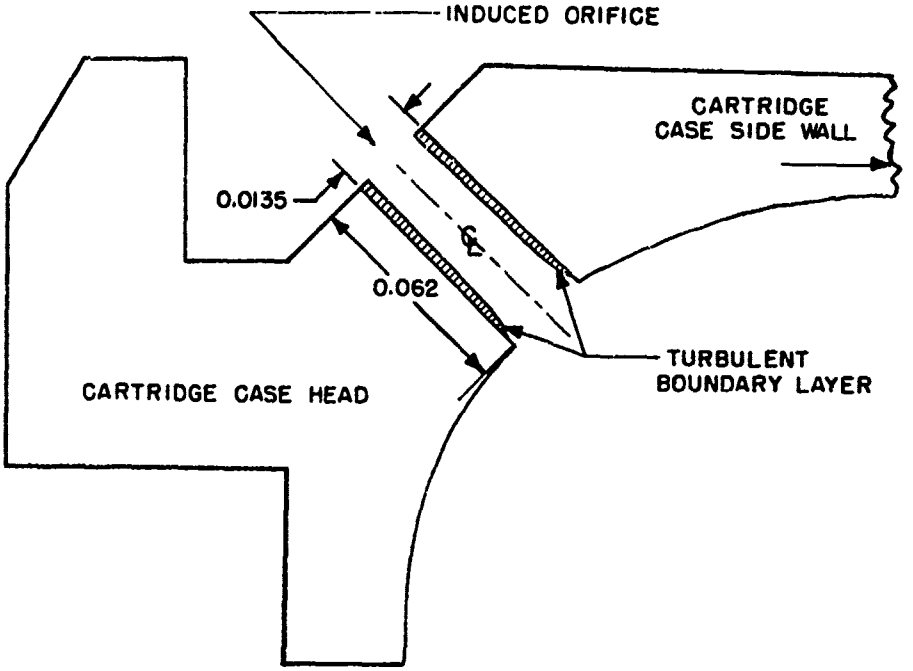

Figure 3. Head Region of 5.56 mm Aluminum Alloy Cartridge Case

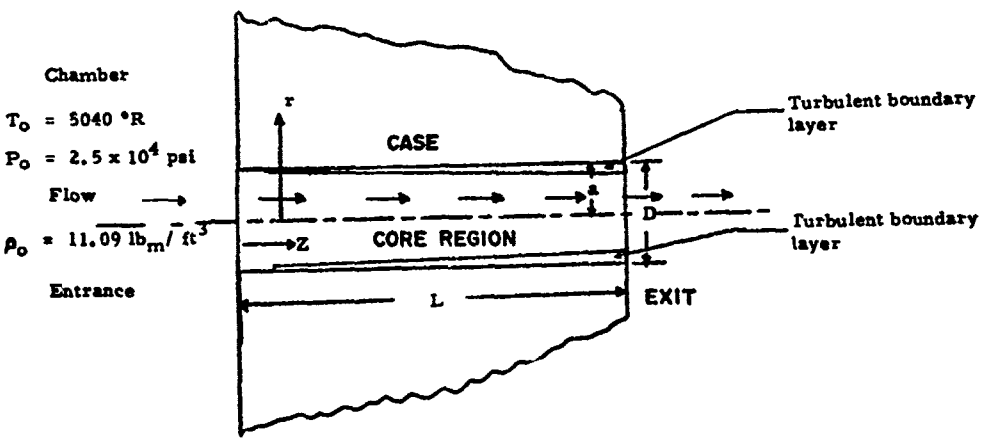

Figure 4. Schematic of Flow Process

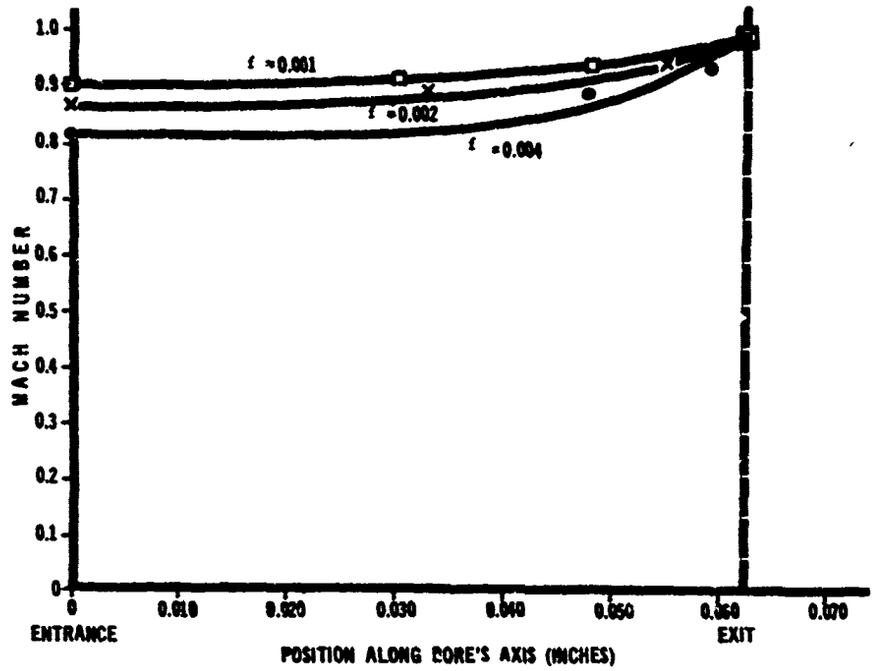

Figure 5. Mach Number as a Function of Position Along the Bore (Friction Factor as Indicated)

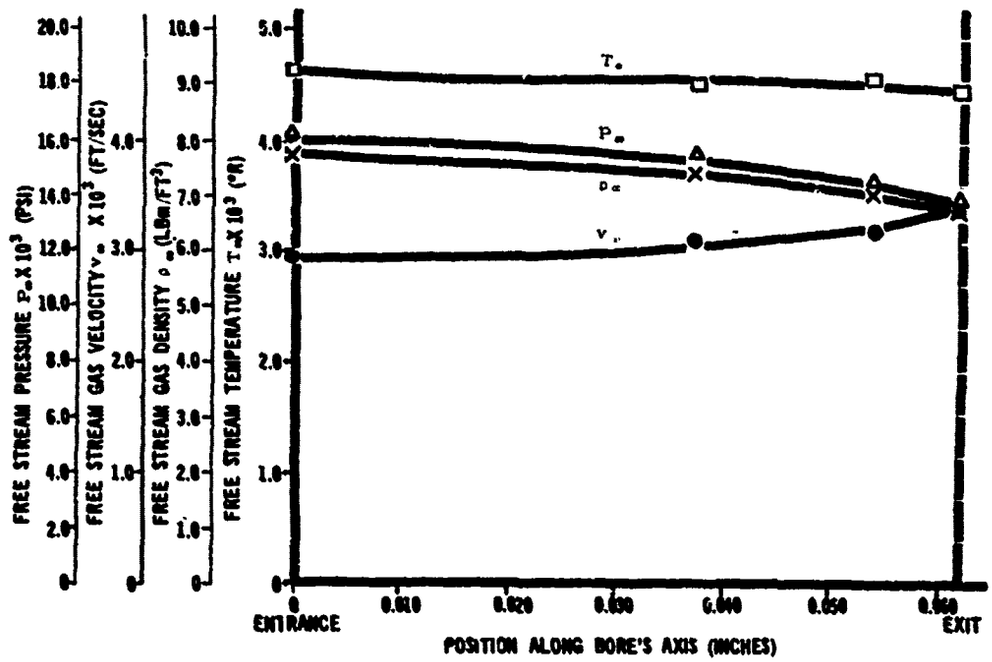

Figure 6. Free Stream Conditions vs Position Along Bore's Axis (f = 0.002)

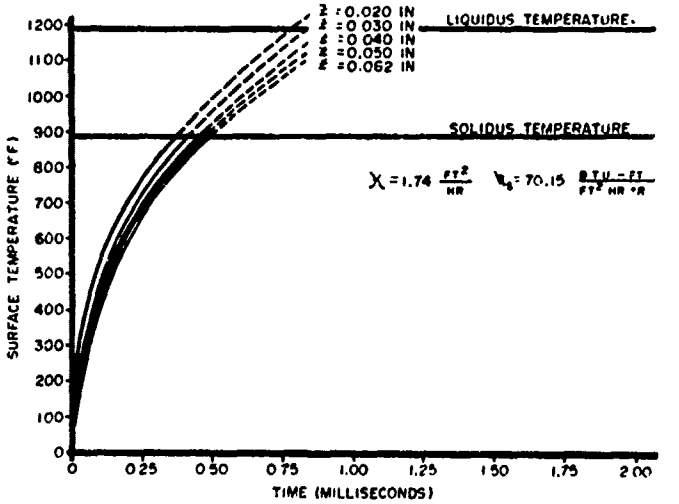

Figure 7. Surface Temperature of Aluminum Bore vs Time (Position as Indicated)

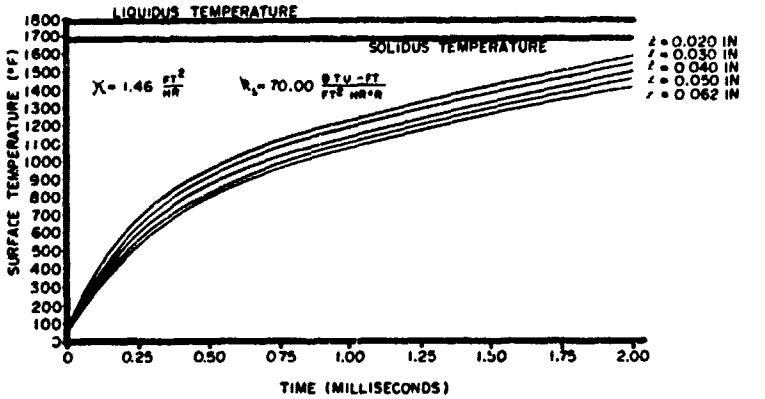

Figure 8. Surface Temperature of Brass Bore vs Time (Position as Indicated)

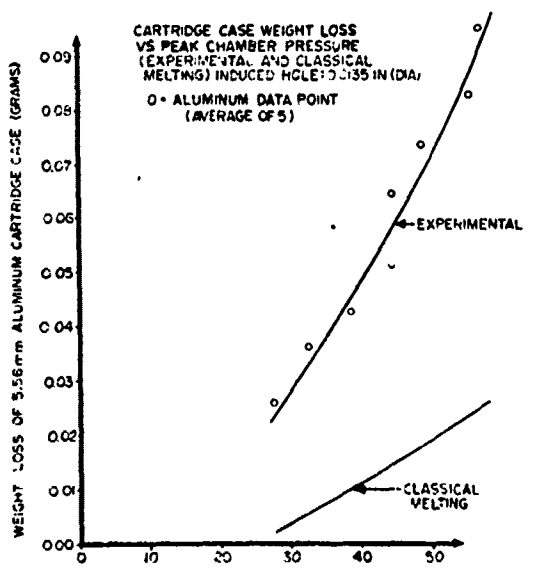

Figure 9. Comparison of Classical Melting Theory and Experiment

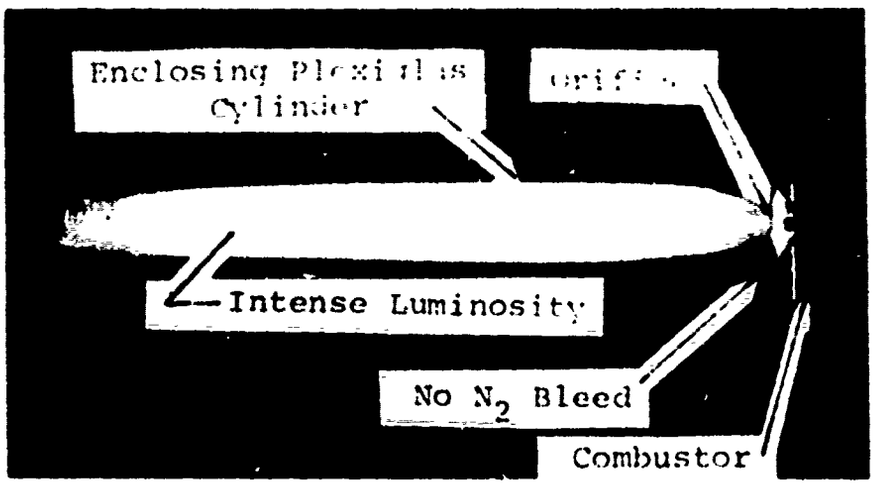

(a) Discharge into Air Environment

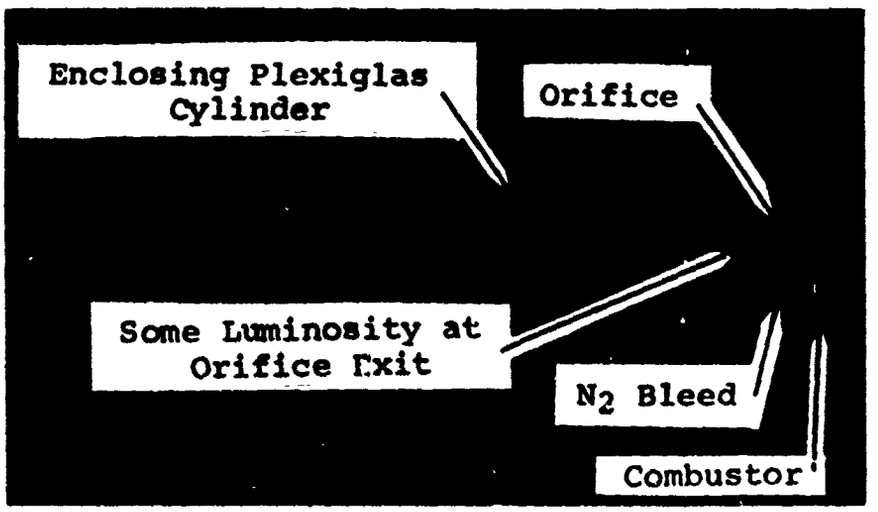

(b) Discharge into Nitrogen Environment

Figure 10. Time Exposed Photographs of the "Burn-Through" Plume into Air and Nitrogen Environments

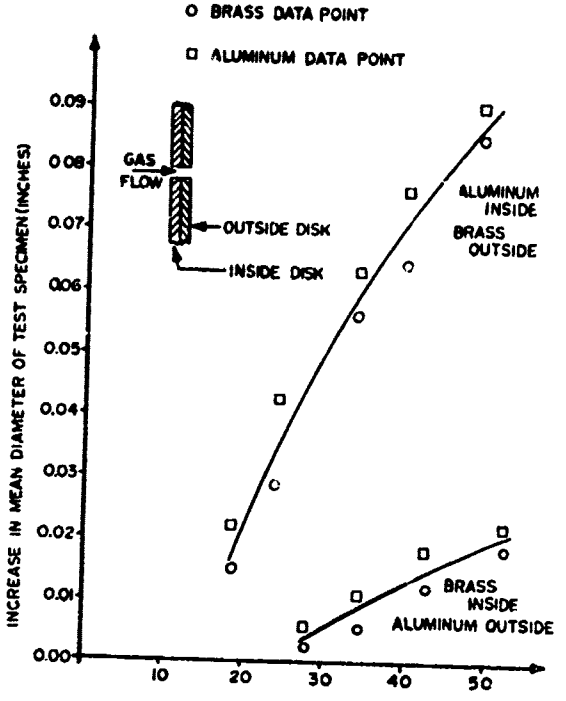

Figure 11. Increase in Mean Diameter of Test Specimens in Double Disk Experiment vs Peak Chamber Pressure

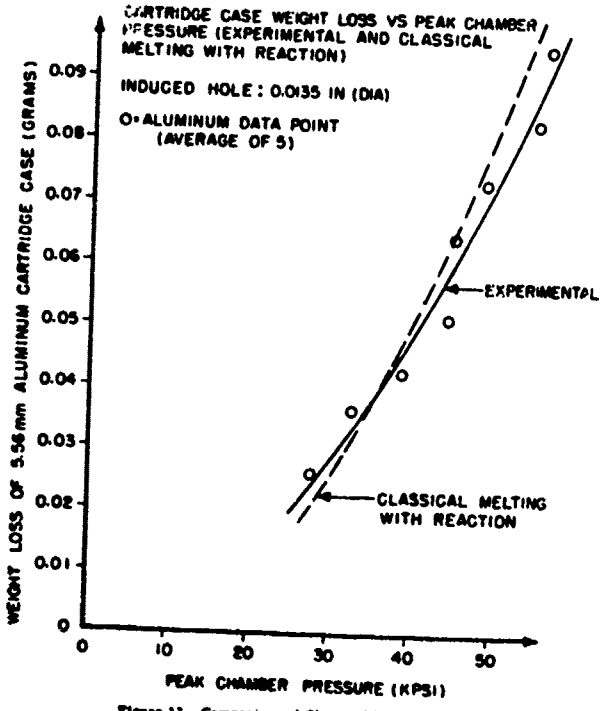

Figure 12. Comparison of Classical Melting Theory with Reaction and Experiment

END